77-80.
7. (a) Hydroformylation: Botteghi, C.; Paganelli, S.; Perosa, A.; Lazzaroni, R.; Uccello-Barretta, G. *J. Organomet. Chem.* **1993**, *447*, 153. (b) Silylation: Brunner, H.; Prester, F. *J. Organomet. Chem.* **1991**, *411*, C1-C2. (c) Norbornadiene used as a masked acetylene: An, Z. W.; Catellani, M.; Chiusoli, G. P. *J. Organomet. Chem.* **1989**, *371*, C51.
8. **3a**: ^{1}H NMR (300 MHz, $CDCl_3$) δ 8.57 (d, 1H, J=5.0 Hz, 6-H in py), 7.59 (t, 1H, J=7.7 Hz, 4-H in py), 7.24 (d, 1H, J=7.7 Hz, 3-H in py), 7.06 (dd, 1H, J=5.3 Hz, 7.4 Hz, 5-H in py), 6.44 (d, 1H, J=11.8 Hz, α-H-C= to py), 6.07-6.15 [s, 2H, 3',4'-Hs in norbornenyl (nbd)], 5.86 (t, 1H, J=11.4 Hz, β-H-C= to py), 2.88-2.96 (m, 1H, 1'-H in nbd), 2.91 (s, 1H, 2'-H in nbd), 2.67 (s, 1H, 5'-H in nbd), 1.51 (d, 1H, J=8.3 Hz, 6'-H in nbd), 1.36-1.43 (m, 3H, 6', 7'Hs in nbd); ^{13}C NMR (75 MHz, $CDCl_3$) δ 156.50, 149.20, 141.97, 137.04, 136.13, 135.70, 127.54, 123.48, 120.96, 48.54, 45.57, 42.12, 37.09, 34.21; MS (m/z) 130 (100), 196 (1.2, M^+-1), 197 (1.3, M^+). **3b**: ^{1}H NMR (300 MHz, $CDCl_3$) δ 8.59-8.63 (m, 1H, 6-H in py), 7.59 (t, 1H, J=7.8 Hz, 4-H in py), 7.18 (d, 1H, J=7.6 Hz, 3-H in py), 7.08-7.15 (m, 1H, 5-H in py), 6.00 (s, 2H, 3',4'-Hs in nbd), 5.60 (d, 1H, J=11.4 Hz, β-H-C= to py), 2.86 (s, 1H, 2'-H in nbd), 2.59 (s, 1H, 5'-H in nbd), 2.16-2.21 (m, 1H, 1'-H in nbd), 2.13 (s, 3H, =C-CH_3), 1.50 (d, 1H, J= 8.02 Hz, 6'-H in nbd), 1.33-1.39 (m, 3H, 6',7'-Hs in nbd); ^{13}C NMR (75 MHz, $CDCl_3$) δ 160.04, 149.13, 136.79, 136.20, 135.68, 135.58, 135.33, 123.25, 121.23, 48.44, 45.51, 42.06, 37.53, 34.38, 23.76; MS 130 (26.3), 144 (100), 145 (33.8), 196 (2.5, M^+-CH_3), 211 (3.8, M^+). **3c**: ^{1}H NMR (300 MHz, $CDCl_3$) δ 8.64 (d, 1H, J=4.8 Hz, 6-H in py), 7.64 (t, 1H, J=7.7 Hz, 4-H in py), 7.12-7.29 (m, 7H, 3,5-Hs in py and Hs in ph), 6.00 (s, 2H, 3',4'-Hs in nbd), 6.12 (d, 1H, J=10.2 Hz, β-H-C= to py), 2.88 (s, 1H, 2'-H in nbd), 2.71 (s, 1H, 5'-H in nbd), 2.18 (dt, 1H, J= 3.1 Hz, 9.46 Hz, 1'-H in nbd), 1.56 (d, 1H, J=8.2 Hz, 6-H in nbd), 1.48 (dt, 1H, J=3.5 Hz, 11.7 Hz, 6'-H in nbd), 1.35-1.42 (m, 2H, 7'-H in nbd); ^{13}C NMR (75 MHz, $CDCl_3$) δ 159.09, 149.53, 137.41, 136.94, 136.12, 135.83, 128.10, 127.18, 126.87, 125.11, 121.62, 48.53, 45.59, 42.16, 38.28, 34.37.
9. Bennett, M. A.; Longstaff, P. A. *Chem. Ind. (London)* **1965**, 846.

Molecular Simulation Studies for Steric Hindrance Effects through the Circular Pore Entrance

Soong-Hyuck Suh*, David Nicholson†, and James M. D. MacElroy‡

Department of Chemical Engineering, Keimyung University, Taegu 704-701, Korea
†Department of Chemistry, Imperial College of Science, Technology and Medicine, London SW7 2AY, U.K.
‡Department of Chemical Engineering, University College Dublin, Dublin 4, Ireland
Received July 18, 1998

The fundamental mechanisms which govern the transport properties of gases, vapors and liquids in porous media are of considerable interests in experimental and industrial applications such areas as membrane separations, heterogeneous catalysis, and gel-permeation chromatography. In many situations, and particularly when the size of pore openings is commensurate with that of diffusing molecules into these microporous materials, the significant hindrance effects can arise during mass transport. This highly localized resistance, more specifically at the pore entrance, is often referred to as a surface barrier effect. Such conditions may cause unusual transport properties, for example, the anomalous non-Fickian diffusivity exhibited in some zeolite and carbon molecular sieves.[1]

In most practical porous materials, there is a spatial variation of pore sizes. Experimental methods are based on the assumption that the absolute size of the pore size distributions can reliably be obtained so that the pore cross-sectional shape is known. However, the experimental extraction of an absolute pore distribution is not straightforward, and this assumption may be seriously in error and lead to large uncertainties especially when micropores are presented. As an extremely useful diagnostic tool, molecular-based computer simulations[2] can provide essentially exact experimental data for precisely defined model systems at the fundamental molecular level. Consequently, molecular dynamics (MD) calculations have been carried out for the analysis of surface barrier effects in a variety of pore systems. Vigne-Maeder *et al.*[3] have performed the dynamic simulations of gas molecules passing through the outer surfaces of aluminum-free MFI- and MOR-type zeolite crystals. More recently, Ford and Glandt[4,5] have undertaken the systematic MD simulation studies of hard-sphere and Lennard-Jones systems for a slit pore mouth model in the dilute gas limit. The simulation approaches using attractive potential fields[3,5] have revealed that the primary mechanism for transport was adsorption followed by surface diffusion to the pore entrance, rather than a direct penetration into a pore from the gas phase.

In the present work, we have reported preliminary MD results of hard-spheres passing through a circular pore mouth which acts as a bottleneck. The individual particle

trajectories are computed by running the conventional hard-core MD simulation.[6] In this algorithm, the positions for the center of the hard-sphere are initially placed inside the range of the circular pore opening, and the velocities are assigned randomly from the subset of the Maxwell-Boltzmann distribution. The trajectories of the particles are advanced until the collision occurs along the line joining the sphere center with the contact point of the circular pore edge. A wall collision is then resolved using the specular boundary reflection conditions, in which the changes in velocities of the colliding spheres are given by the requirement of linear momentum and energy conservations. All MD simulations were carried out by performing at least 20 million test particles in a given condition, and, for very small pore systems, as many as 200 million independent trajectories were tracked.

In Figure 1, the log-log plot for the total fraction of successful escapes, f_{esc}, is illustrated as a function of the reduced circular pore diameter, D^*.($D^*=D/\sigma_H$ and σ_H is the hard-sphere diameter.) In all cases studied, the error bars, computed from the standard deviation among 20 independent samples, were typically smaller than the symbol size itself. Also shown in this figure as the chain-dotted curve are the previous MD results, reported by Ford and Glandt,[4] for the system of specularly scattering hard-spheres through the rigid slit entrance. Their simulation data, analytically given by a sixth-order polynomial expression, were scaled as having the slit pore gap of width, $h^*(h^*=h/\sigma_H)$, equal to the circular pore diameter, D^*.

Computations obtained from both pore systems exhibit strong dependencies on cross-sectional variation across the entire range of pore opening conditions investigated here.

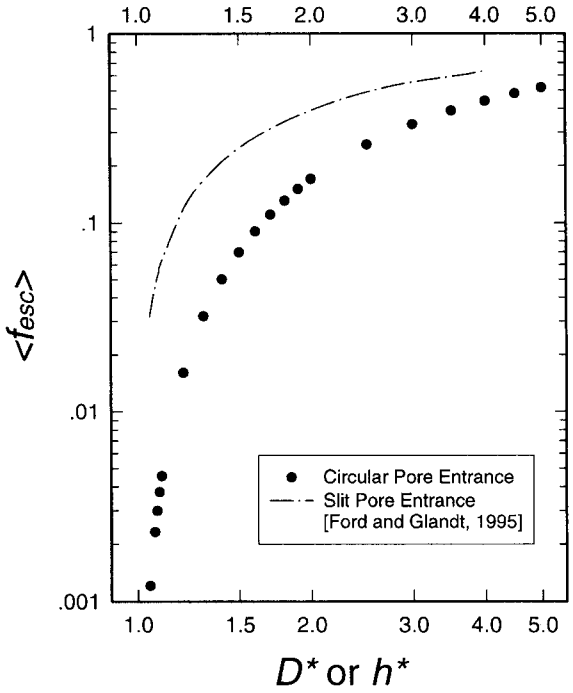

Figure 1. A log-log plot for the total fraction of successful escapes as a function of the reduced circular pore diameter. Also shown as the chain-dotted curve is the simulation data for hard-spheres passing through the slit pore entrance.

Similar to the slit pore case, MD results for the circular pore mouth are seen to be strongly non-linear decaying function, particularly when the diffusing molecular size approaches the characteristic pore size. Comparing the slit and the circular pore systems shows that an increased curvature at the pore opening causes more hindrance of molecular pathways as they diffuse toward the pore opening. In contrast to the two-dimensionally restricted trajectories in the circular pore, molecular motions may gain relatively free mobilities in the slit pore which is blocked in only one dimension. This indicates the influence of geometric effects not only by the characteristic pore length but also by the pore cross-sectional shape.

We may assume that the rate of passage through the pore bottleneck is proportional to its cross-sectional area. This may be true only in the ranges of very wide pore openings. For the ranges of $D^*\geq 3.0$ or greater, the resulting simulation values increase monotonically with increasing the pore size. However, even for the case of $D^*=5.0$, it was observed a large discrepancy from the predicted value, based on the constant passage rate, which accounts for only a direct passage across the pore entrance region. Our MD results show that, in the region where the size of a penetrating molecule is close to that of the pore circular opening, the escaping probabilities indeed vary an order of magnitude difference with respect to the small variations for D^*, for instance, $f_{esc}=0.00121$ and 0.0161 for $D^*=1.05$ and 1.2, respectively.

There are two basic phenomena that contribute to the escaping probability in such purely entropic systems: the size-exclusion hindrance and the velocity screening effects. The first one is related to the effective free area which accounts for the non-zero size of diffusing molecules. In addition to the steric hindrance effect, the dynamic feature which can be connected with the boundary scattering mode during the collision processes is also involved. In this latter way, molecules with certain velocity characteristics are screened out and cannot penetrate into the interior pore region. For specular boundary reflection conditions, successfully passing molecules should have, during all collisional trajectories, a positive value of the post-collisional velocity component along the flow direction normal to the pore opening. Otherwise, molecules will be eventually reflected away from the pore wall.

In such a purely entropic model pore, the mass transfer coefficient, k_H, may be expressed as

$$k_H = f_{esc}\,\frac{A_{entr}}{A_{tot}} \tag{1}$$

where A_{entr} and A_{tot} represent the surface area of the pore entrance and the total surface area based on a single-pore geometry, respectively. This property is, by definition, a single-particle transport property. It is worth noting that the temperature dependence is irrelevant for non-interacting pore systems. The diffusing trajectories emitted from any point on the internal pore surface are linear, and the duration of trajectories does not affect the molecular penetrating fraction or the mass transfer coefficient.

Our MD calculations can be used to make predictions of the mass transfer ratio (or selectivity) for multi-component systems. We consider here a binary mixture of hard-sphere

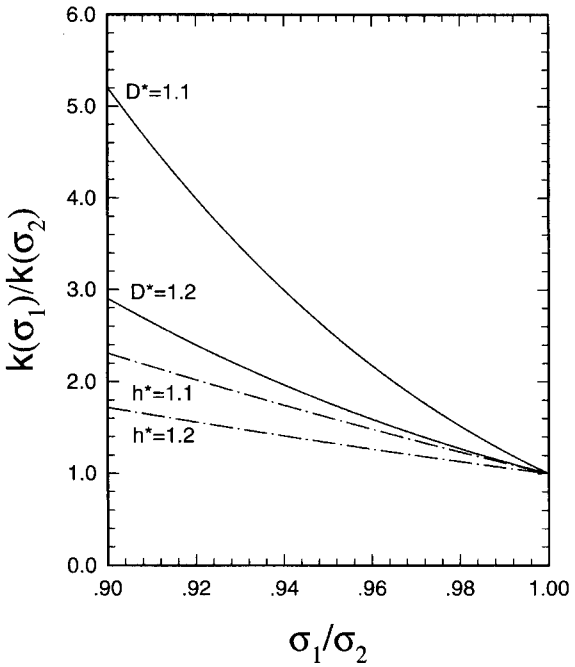

Figure 2. Mass transfer ratio (or selectivity) for a binary mixture of hard-sphere fluids as a function of the size ratio. The solid and the chain-dotted curves represent the resulting coefficient for the circular and the slit pore entrance, respectively.

fluids with a small species of diameter σ_1 and a large species of diameter σ_2. Under these conditions, the mass transfer ratio is simply related to the escaping ratio of two different species in a given value of pore size. In Figure 2, the resulting mass transfer coefficients are plotted for the two sets of D^*=1.1 and D^*=1.2 as a function of the penetrant size ratio, σ_1/σ_2, in order to illustrate the size and shape dependencies on mass transfer selectivities. The solid and the chain-dotted curves, respectively, represent the resulting coefficients for the circular and the slit pore openings.

It is the expected trend that the larger size ratios lead to the larger mass transfer selectivities, and such size-dependent selectivities disappear in the limit of $\sigma_1 \rightarrow \sigma_2$. As can be seen in this figure, dramatic changes in selectivities are displayed with respect to the pore cross-sectional variations, and the geometric effects become more profound in the circular pore system. For the small pore openings, the relatively small changes in penetrant size ratios result in significant differences in the mass transfer resistance due to the complexities coupled with the geometric hindrance and the velocity screening effects in this regime. This large selectivity obtained in our MD calculations is in qualitative agreement with theoretical and simulation studies which suggest that quite minor changes in pore geometry may lead to significant modifications in the diffusive behavior of microporous systems.

The above observations are not restricted to the free molecular (Knudsen) regime. Similar conclusions have also been obtained from the simulation studies of dense fluid systems. As demonstrated in the systems of hard-sphere[7,8] and Lennard-Jones[9,10] fluids confined in the sequentially linked sphere-cylinder pore, apparent packing effects are exhibited near the pore entrance region and the pore fluid experiences structural reordering in the axial pore direction for higher concentrations. Although our simple pore model only represents the conceptual nature of idealized systems, the structural geometries of some zeolite cavities closely resemble such model systems. The pore size dependencies investigated in this work would be useful in gaining a better understanding of how effectively the modification of pore geometries influences molecular diffusion processes. It would be of interest to extend to more realistic pore systems in the presence of adsorption force fields in order to verify a number of the conclusions observed in our MD studies.

Acknowledgment. This research is financially supported by the Korea Science and Engineering Foundation (CAPT, 1997). SHS is grateful to the Imperial College of Science, Technology and Medicine for their hospitality during the period when this work was carried out.

References

1. Karger, J.; Ruthven, D. M. *Diffusion in Zeolites and Other Microporous Solids*; Wiley: New York, U. S. A., 1992.
2. Allen, M. P.; Tildesley, D. J. *Computer Simulation of Liquids*; Clarendon Press: Oxford, U. K., 1987.
3. Vigne-Maeder, F.; El Amrani, S.; Gelin, P. *J. Catal.* **1992**, *134*, 536.
4. Ford, D. M.; Glandt, E. D. *J. Membrane Sci.* **1995**, *107*, 47.
5. Ford, D. M.; Glandt, E. D. *J. Phys. Chem.* **1995**, *99*, 11543.
6. Alder, B. J.; Wainwright, T. E. *J. Chem. Phys.* **1959**, *31*, 459.
7. Suh, S.-H.; Lee, Y.-T.; MacElroy, J. M. D. In *Discussions on Zeolite and Microporous Materials*; Chon, H.; Uh, YS Ed.; Hanrimwon: Korea, 1997; p 283.
8. Suh, S.-H.; Heo, N.-H.; Nicholson, D. *J. Chem. Eng. Jpn.* **1998**, (in press).
9. Demi, T.; Nicholson, D. *J. Chem. Soc., Faraday Trans.* **1991**, *87*, 3791.
10. Demi, T.; Nicholson, D. In *Studies in Surface Science and Catalysis*; Suzuki, M. Ed.; Elsevier: Amsterdam, The Netherlands, 1993; Vol. 80, p 137.